Food Control 107 (2020) 106778

Contents lists available at ScienceDirect

Food Control

journal homepage: www.elsevier.com/locate/foodcont

Modeling the temperature-dependent microbial reduction of *Enterococcus faecium* NRRL B-2354 in radio-frequency pasteurized wheat flour

Jie Xu, Ren Yang, Yuqiao Jin, Graham Barnett, Juming Tang*

Department of Biological Systems Engineering, Washington State University, Pullman, WA, 99164-6120, USA

ARTICLE INFO

Keywords:
Radio-frequency heating
Enterococcus faecium
Microbial validation
Wheat flour
Bigelow model

ABSTRACT

Radio-frequency (RF) pasteurization has been identified as a potential technology to pasteurize low-moisture foods. Recent studies demonstrated that soft wheat organic flour with water activity of 0.45 at 25 °C subjected to RF heating at 80–85 °C followed by 10–25 min nature cooling could result in 2.5–3.7 $\log_{10}$ reduction of *Enterococcus faecium* NRRL B-2354 (*E. faecium*), a valid surrogate for *Salmonella* Enteritidis PT30. Bigelow model was used to predict the temperature-time dependent microbial reduction of bacteria during a RF process. However, reported studies only validate the accuracy of this model by testing microbial reductions of target microorganism at limited locations and at a fixed heating rate. RF processing with a natural cooling may lead to a relocation of the least lethality zone, which could fail in predicting the worst scenario. In this study, microbial reduction of *E. faecium* was evaluated at 15 locations (evenly distributed in top, middle and bottom layers) in a 1.8 kg-wheat flour container (water activity 0.45 ± 0.02 at 22 °C) after RF heating to 80 °C with three different RF heating rates (36.0, 11.3, 5.5 °C·min^{-1}), followed by a 20 min nature cooling. Fiber optic sensors were used to monitor the temperatures at the geometric center of three layers throughout the process. Bigelow model was applied to predict the temperature-time dependent reductions of *E. faecium* in each layer. RF heating to 80 °C combined with a 20 min nature cooling could achieve an average microbial reduction of 1.21–4.64 $\log_{10}$ CFU/g in wheat flour at water activity 0.45 ± 0.02 at 22 °C. Fast-heating rate resulted in non-uniformity in terms of temperature and inactivation. Using least sum of squares technique, Bigelow model yielded *D*-value of 8.3 min at 80 °C with a given *z*-value of 11.7 °C. The fitting results using the Bigelow model were in good agreement with that from the experiment (R^2 = 0.81). This study provides comprehensive evidence on using Bigelow model to predict the real-time microbial reduction of bacteria in a RF process.

1. Introduction

Radio-frequency (RF) heating has been used for drying, defrosting products in the food industry for many years (Mermelstein, 1998; Piyasena, Dussault, Koutchma, Ramaswamy, & Awuah, 2003). Recently, RF heating was found to be a potential approach for postharvest disinfection or pasteurization of low-moisture foods to minimize safety risk since its ability to fast heat up bulk low-moisture products without impairing organoleptic quality (Wang, Monzon, Johnson, Mitcham, & Tang, 2007b, 2007a; Hou, Kou, Li, & Wang, 2018; Hu, Zhao, Hayouka, Wang, & Jiao, 2018; Jiao, Johnson, Tang, & Wang, 2012; Wang, Tiwari, Jiao, Johnson, & Tang, 2010). Reducing temperature variations in RF heated samples is essential for quality and pathogen control. Many researchers have attempted to improve the temperature uniformity of RF heating (Birla, Wang, Tang, & Hallman, 2004; Jiao, Shi, Tang, Li, & Wang, 2015; Villa-Rojas, Zhu, Marks, & Tang, 2017).

Identification and validating the lowest lethality zone are critical in developing effective thermal treatments for commercial operations. Microbial validation of RF processes is challenging since pathogenic bacteria (such as *Salmonella* spp.) cannot be directly introduced into food processing environments (Niebuhr, Laury, Acuff, & Dickson, 2008). In this case, microbial validation test using inoculated surrogate packs is a practical way to avoid cross-contamination (Liu, Ozturk, et al., 2018; Podolak & Black, 2017). In previous studies, microbial reductions of *Escherichia coli* ATCC 25922 on corn grains, *Enterococcus faecium* NRRL B-2354 in wheat flour, or *Aspergillus* parasiticus on in-shell almonds were monitored at limited locations, such as the geometric center or other representative locations (Li, Kou, Cheng, Zheng, & Wang, 2017; Xu, Liu, et al., 2018; Zheng, Zhang, & Wang, 2017). For instance, Liu (Liu, Ozturk, et al., 2018) placed a 5 g-bag of sample inoculated with *Salmonella* or *E. faecium* at the geometric center of a treated container with 3.0 kg wheat flour for RF microbial validation.

* Corresponding author.
E-mail address: jtang@wsu.edu (J. Tang).

https://doi.org/10.1016/j.foodcont.2019.106778
Received 16 March 2019; Received in revised form 16 July 2019; Accepted 17 July 2019
Available online 18 July 2019
0956-7135/

Wei (Wei, 2017) embedded a 20 g-polyethylene bag of the inoculated sample at the center of the top surface of black peppercorn and ground black pepper to represent the worst scenario during RF heating. The least heated zone of treated sample in a rectangular container during RF heating has been identified at the geometric center (Liu, Ozturk, et al., 2018), or the center on the top surface (Kim, Sagong, Choi, Ryu, & Kang, 2012). However, in industrial processes, products after RF treatments are commonly cooled down naturally in the air to save energy and obtain sufficient microbial reduction. Thus, the location of the lowest lethality zone of RF treated samples after a natural cooling might change due to heat conduction and ambient heat loss. In this case, monitoring the survival of target microorganism at one location might fail in giving a conservative safety margin of RF treated materials.

It is acknowledged that during an isothermal treatment, the population of microorganisms decreases exponentially with treatment time at a given temperature in aqueous environments. Thus, the microbial reduction follows a first-order reaction that can be modeled by the Bigelow model and Arrhenius equation (Bigelow, Bohart, Richardson, & Ball, 1920; Bigelow & Esty, 1920). Recent studies also found the linear relationship between $\log_{10}D$-value of bacteria and treatment time in low-moisture foods, including wheat flour, almond flour, and non-fat milk powder (Villas-Rojas, 2015; Liu, Rojas, Gray, Zhu, & Tang, 2018; Liu, Tang, Tadapaneni, Yang, & Zhu, 2018; Xu, Tang, et al., 2018). The temperature-dependent microbial reductions of *Salmonella* and *E. faecium* have been predicted by Bigelow model, based on the measured temperature profiles and microbial thermal resistance parameters (Liu, Ozturk, et al., 2018; Xu, Liu, et al., 2018). However, the Bigelow model was only verified by survival data at one location under a fixed RF heating rate. The application of using Bigelow model to fit survival data of *E. faecium* at other locations of the treated sample and different RF heating rates has not been investigated systematically.

The overall aim of this study was to use Bigelow model to predict the temperature-time microbial reduction in a RF pasteurization process and validate this model by monitoring the microbial populations of *E. faecium* at multiple locations in wheat flour (water activity 0.45 ± 0.02 at 22 °C) at different RF heating rates. The specific objectives were to: 1) develop a temperature measurement system for heating uniformity evaluation; 2) evaluate the influence of heating rate on temperature uniformity of RF heating; 3) investigate the survival of *E. faecium* in wheat flour at 15 locations after RF heating to 80 °C followed by a 20 min natural cooling; and 4) test the fitness of the Bigelow model to verify its potential in industrial applications.

2. Materials and methods

2.1. Food sample

In this study, soft organic wheat flour (Eden Foods, Clinton, MI) was used as a model food due to its relationship with outbreaks and previous studies by the same group (Liu, Ozturk, et al., 2018; Villa-Rojas et al., 2017; Xu, Liu, et al., 2018). The average particle size of wheat flour measured by an ATM sonic sifter (ATM Corporation, Milwaukee, WI) was 144 ± 60 μm, with background microflora 1.92 ± 0.15 $\log_{10}$ CFU/g. The nutritional composition of the wheat flour sample is reported by (Liu, Ozturk, et al., 2018). Since water activity (a_w) is an essential factor influencing RF heating uniformity as well as thermal resistance of bacteria (Jiao, Tang, & Wang, 2014; Syamaladevi et al., 2016; Zhang, Zhu, & Wang, 2015), a_w of wheat flour was adjusted from 0.32 (initial a_w) to 0.45 at room temperature (~22 °C) by adding sterilized Milli-Q water, with corresponding moisture content 12 g H_2O/100 g sample. a_w of wheat flour was measured by a water activity meter (AUQA PRE, Meter Group, Pullman, WA, USA). Moisture-adjusted wheat flour was mixed manually to ensure the moisture of sample was uniform and then, sealed in a closed container for 1 h at 22 °C before treatment.

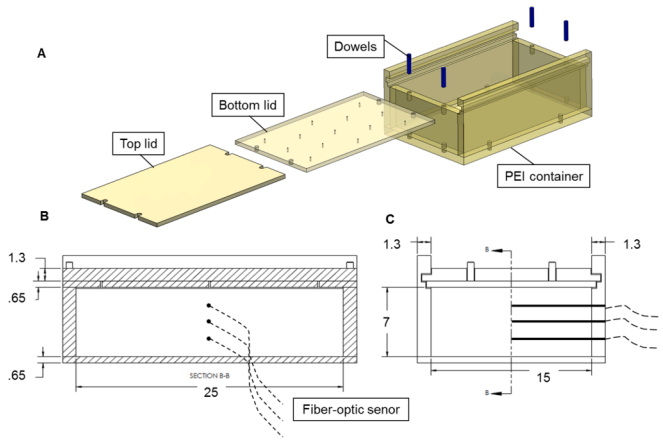

Fig. 1. (A) 3D dimension of RF heating container, (B) lateral view, (C) cross-section view of the container with fiber-optic sensors in three layers. Dimensions in cm.

2.2. Design of the RF heating container and real-time temperature monitoring strategy

A rectangular sample container was made from polyetherimide (PEI) for the RF treatments. The inner dimension of the container was 25 × 15 × 7 cm^3 (L × W × H) (Fig. 1A). Two lids were overlapped to minimize heat loss during measurement. The top lid was placed on for processing and then removed for temperature measurement. The bottom lid was manufactured with 13 small holes for different configurations of thermocouple probes. A stepped groove was designed for sliding the lids and four dowels made with PEI were used for easy assembly (Fig. 1A).

On one long side of the container, three holes were predrilled at different height to allow the placement of fiber-optic sensors to measure temperatures in three different layers of the sample (Fig. 1B and C). Pre-calibrated fiber-optic sensors (OpSens TempSens, OpSens Inc., Quebec, Canada) connected to a multi-channel fiber-optic probe temperature-monitoring device (OpSens TempSens, OpSens Inc., Quebec, Canada) were used to record temperatures during RF treatment.

2.3. Design of thermocouple platform for temperature measurement during cooling

A thermocouple platform was designed and manufactured by the Engineering Shop of Voiland College of Engineering and Architecture (Washington State University, Pullman, WA, USA) to measure the end-point temperatures in different locations of the sample after RF treatments. The detailed design of the thermocouple platform is shown in Fig. 2A. Double-deck boards with multiple holes were designed to allow for placement flexibility and future system expansion. Type K thermocouple probes (with 0.32 cm grounded sheath, Omega, Stamford, CT, USA) were aligned on the board and passed through the container to reach the measurement location. Locking handles and external springs were designed to enable handlers to press down thermocouple probes at varying levels.

For each measurement, the container was taken out from the RF system right after RF heating. Then, the platform was loaded on the container with pins down for better alignment (Fig. 2A). In this study, 13 type-K thermocouple probes were numbered and distributed evenly (Fig. 2B). Temperature measurement was performed for one layer each run. During the measurement, the thermocouple platform was pushed down and locked with handles at a desired level for at least 20 min. Once the measurement was completed, the locking handles were released and moved back to the initial position. A separate RF heating with fresh samples were conducted for the other two layers. In total, 6

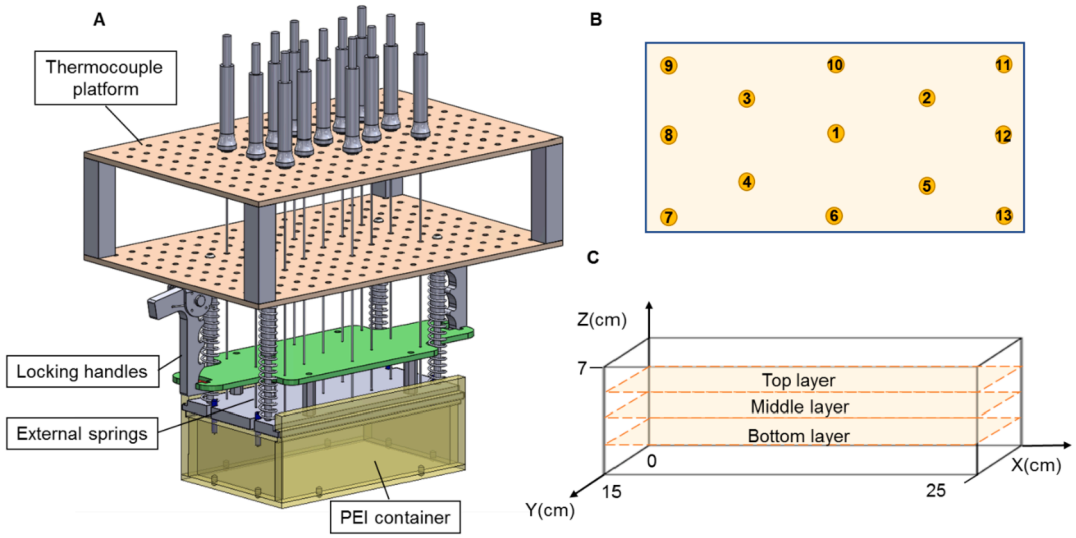

Fig. 2. (A) Design of temperature measurement system, (B) top view of 13 locations for temperature measurement, (C) three temperature measurement layers in the container with filled wheat flour.

RF heating tests were conducted at the same heating rate, with two independent replicates for each layer.

2.4. RF heating system

The RF system used in this study was a pilot-scale, 27.12 MHz, 6 kW free-running oscillator system (COMBI 6-S, Strayfield International, Wokingham, UK). The detailed information of the RF system was described in (Wang et al., 2010). In this study, three electrode gaps (10.2 cm, 11.4 cm, 12.7 cm) were selected to achieve the heating rate of 36.0, 11.3, 5.5 °C·min^{-1}, respectively. At each heating rate, the container with 1.8 kg preconditioned wheat flour was placed on the stationary conveyor belt at the center of the bottom plate between the two electrodes to obtain the best uniformity (Huang, Zhu, Yan, & Wang, 2015; Ozturk, Kong, Trabelsi, & Singh, 2016). The container filled with wheat flour was firstly heated up to 80 °C by RF energy and then naturally cooled down in the RF oven for 20 min. The tests were completed in duplicate for each heating rate.

2.5. Microbial reduction of surrogate during RF treatment

2.5.1. Culture preparation

Enterococcus faecium NRRL B-2354 (*E. faecium*) was obtained from the University of California, UC-Davis and stored as a frozen stock in tryptic soy broth (TSB) with 20% (vol/vol) glycerol. The detailed inoculation procedure was described in Villa-Rojas et al. (2013). Briefly, *E. faecium* was resuscitated in TSB supplemented 0.6% yeast extract (TSBYE) for two successive transfers and incubated at 37 °C for 24 h. Then, 1 mL of the previous culture was transferred to tryptic soy agar with 0.6% yeast extract (TSAYE) plate (150 mm × 15 mm, dia × height) and incubated at 37 °C for 24 h. The bacterial lawn from four TSAYE plates was harvested by 0.1% peptone water and then centrifuged at 6000 × *g* for 15 min at 4 °C. The supernatant was discarded and the bacteria pellet was re-suspended with 3 mL of 0.1% peptone water for inoculation (~10 $\log_{10}$ CFU/mL).

2.5.2. Preparation of inoculated packs

One mL of re-suspended bacterial culture was mixed with 10 g wheat flour until visible clumps disappeared. Then, 10 g of the inoculated sample was inoculated with 90 g more wheat flour. The inoculated sample was equilibrated in a Hotpack 435315 humidity chamber (SP Industries, Inc., Warminster, PA, USA) for a minimum of 4 days at 22 °C to reach the target water activity (a_w 0.45 ± 0.02 at 22 °C) (Hildebrandt et al., 2016).

The previous study showed that the embedded small packs would not influence the heating profile of RF treated sample (Liu, Ozturk, et al., 2018). Two grams of inoculated sample was sealed in a sterilized round-shape Whirl-Pack bag (Fig. 3A). The weight of the sample pack (2 g) was maximally reduced to minimize its influence on the heating uniformity of treated sample during RF heating.

2.5.3. Sample loading

During sample loading, the container was put on a balance and tared the weight. A proper amount of un-inoculated wheat flour (described in 2.1) was firstly loaded to the height of the bottom layer. Five sample bags were then placed at the center and four corners (Fig. 3B). More wheat flour was added to the height of the middle and top layer (with five packs at each layer) until the total weight reached to 1.8 ± 0.3 kg. Since the density of flour can influence the dielectric properties of treated samples, the same amount of flour (1.8 ± 0.3 kg) followed with 10 taps was performed each time during filling. A straight edge was used to flatten the sample surface before closing the container.

2.5.4. Experimental procedure

During RF treatments for samples with embedded inoculated packs, a fiber-optic sensor was placed to measure the temperature of the center in each of the three layers (top, middle, and bottom as shown in Fig. 1B and C). RF heating was stopped when the middle sensor read 79.5 °C. Under each heating rate, the survivor population of *E. faecium* was determined at two points: the end of RF heating, and the end of 20 min natural cooling. Immediately (within 30s) after each treatment, 15

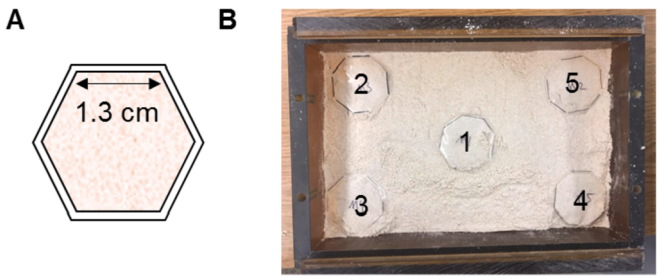

Fig. 3. (A) Sample pack with 2 g of inoculated wheat flour, (B) Top view of five locations for inoculated packs in each layer.

inoculated sample packs were removed and cooled down in ice water for 3 min to stop the inactivation process.

For enumeration, 1 g of randomly selected flour from each treated pack was transferred to 9 mL peptone water and stomached at 230 rpm for 3 min. Ten-fold serial dilution was performed and the properly diluted sample was spread plated on differential media for *E. faecium* (TSAYE supplemented with 0.05% ammonium iron (III) citrate and 0.05% esculin). Plates were incubated at 37 °C for 24 h and the typical colonies with black center were counted as survivors. The number of survivors was transferred into $\log_{10}$ CFU/g. The average survivors from two independent replicates at each heating rate were used as the results.

2.6. Model applications

2.6.1. Heating uniformity

The temperature uniformity can be indicated by the uniformity Index (UI), which referred to an equation that was defined previously (Alfaifi, Tang, Rasco, Wang, & Sablani, 2016):

$$UI = \frac{1}{(T_{ave} - T_{initial})V_{vol}} \int_{V_{vol}} \sqrt{(T - T_{ave})^2 dV_{vol}} \quad (1)$$

where T and T_{ave} are local and average temperature (°C) inside the food sample over the volume (V_{vol}, m^2), $T_{initial}$ is the initial average temperature (°C) of treated food before RF heating. The smaller the UI value, the better the RF heating uniformity. In this study, UI was determined and compared for each layer at each RF heating rate. UI was calculated by using temperature data measured by type-K thermocouple probes at 13 locations.

2.6.2. Model prediction

Bigelow model (Equation (2)) was applied to fit the microbial results from the experiment by trying different D_{Tr}- and z-values to obtain the best fit. This model has been extensively used for processing design in the canning industry. It has also been recently applied on low-moisture foods for conservative prediction of microbial reductions of bacteria in RF pasteurized wheat flour (Liu, Ozturk, et al., 2018; Xu, Liu, et al., 2018).

$$Log\frac{N_0}{N_t} = \frac{1}{D_{Tr}} \int_0^t 10^{\frac{(T(t)-Tr)}{z}} dt \quad (2)$$

where N_t and N_0 are the survival population of target microorganism at time t and 0, $T(t)$ is the measured real-time temperature. T_r is the reference temperature (80 °C), z and D_{Tr} are thermal resistance parameters of *E. faecium* in wheat flour (a_w 0.45 at 22 °C).

3. Results and discussion

3.1. Temperature history profile during RF process

Fig. 4 shows the temperature history profiles of wheat flour (measured at the geometric center of the top, middle, and bottom layers) at three RF heating rates. The heating time, which was the time for the geometric center to reach 80 °C at three heating rates (36.0, 11.3, 5.5 °C·min^{-1}), were about 100s, 310s, 650s, respectively. After a 20 min natural cooling, temperatures of the treated sample declined around 5 °C for all experimental setups.

The sample means, maximum and minimum temperatures recorded by fiber-optic sensors during cooling section are summarized in Table 1. The average temperature variation among three measured layers was 6.1, 4.2, and 3.4 °C under the heating rates 36.0, 11.3, 5.5 °C·min^{-1}, indicating a negative effect of fast heating rate on heating uniformity in a cross-sectional direction. The average temperature in the middle layer was the highest, followed by the top and bottom layer. The middle layer of the sample was also mostly heated during RF heating because of the concentrating electric field (Huang et al., 2015; Wang, Monzon, Johnson, Mitcham, & Tang, 2007a). Previous study also found that temperature values were higher at the middle layers and corners were more heated than centers of RF heated wheat flour (Tiwari, Wang, Tang, & S. Birla, 2011). The average sample temperature in the bottom layer was the lowest in this study, and that might be caused by the direct contact of the treated container to the bottom electron. The average temperature in the top layer was lower than that in the middle layer properly because of the evaporative cooling. A previous report observed the lowest temperature was on the top surface when the treated sample was uncovered and exposed to air (Huang et al., 2015).

3.2. RF heating uniformity

Infrared camera is commonly used to measure the surface temperature of RF treated sample (Birla et al., 2004; Ozturk, Kong, Singh, Kuzy, & Li, 2017; Wang et al., 2007a). An infrared camera is convenient to use when the sample can be easily separated into layers (Birla et al., 2004; Wang et al., 2007a). But, applying this technique to measure temperatures of powders was challenging, since it required special design of separated box spaces, which may affect the pack density of the sample and cause heat loss. The thermocouple platform developed in this study was used to determine the heating uniformity of wheat flour and similar products after RF treatment, and it was more convenient compared with an infrared camera.

The thermocouple probes took around 90 s to obtain a stable reading. In this case, the temperature data at 90s and at 1200s was used to calculate the temperature variation (ΔT) and UI at each layer. The advantages of using thermocouples for temperature measurement were: 1) temperature history profiles can be recorded at multi-locations simultaneously; 2) the temperature distribution can be identified easily with clear identification of cold/hot spot, and 3) the temperature profile can be measured for both the sample surface and interior within the container. However, the disadvantages included: 1) the come-up-time (CUT ~ 90s), which was the time in seconds for the thermocouple probe to get a stable reading, was longer than that of a fiber optic sensor; 2) the heat loss from the thermocouple probes to the surrounding air during measurement caused a consistently lower temperature value compared to that of a fiber-optic sensor (data not shown); 3) powder density influenced the reading accuracy, e.g., the bottom layer always had the highest temperature, while the top layer (least sample attachment) had the lowest temperature; 4) thermocouple probes were only able to measure the temperature during natural cooling, not during RF heating since metal probes cannot function in the RF field. In this case, the data obtained from the thermocouple probes right after RF heating and 20 min cooling were used only as a reference for assessing temperature variation and heating uniformity.

The temperature data for each layer is shown in Table 2. From Table 2, the temperature variation within a single layer was the highest in the top layers regardless of the heating rate. In terms of heating uniformity, the top layer had the highest UI number (worst heating uniformity), while for middle and bottom layers, the UI index decreased with the decrease of heating rate, indicating the slower the heating rate, the better heating uniformity of a RF process. This was inconsistent with a previous finding that the RF heating rate has an adversely affect on heating uniformity because of rapid and run away heating (Ozturk et al., 2017).

3.3. Microbial reduction after RF heating

The microbial reduction of *E. faecium* was determined at 15 locations in the container at each heating rate. Less than 2 $\log_{10}$ CFU/g population reduction was achieved after RF heating in all circumstances (Fig. 5). The inoculated packs at the middle layer had the highest, but no significantly different microbial reduction compared with that of the top and bottom layers.

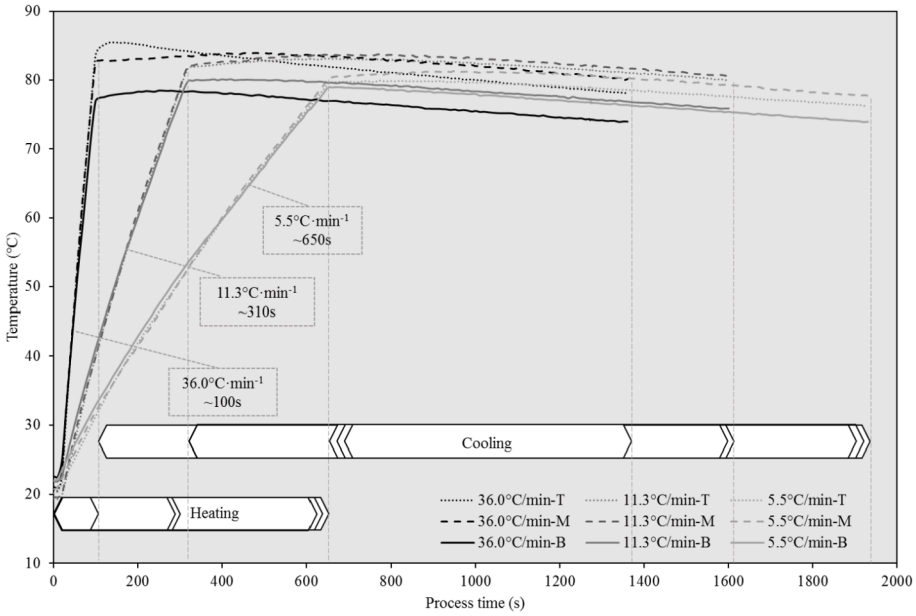

Fig. 4. Temperature history profile of wheat flour subjected to RF heating with a 20 min natural cooling for three different heating rates with corresponded heating times in second. The type of line shows three measured locations (dot line: the top layer, T; dash line: middle layer, M; solid line: bottom layer, B).

Table 1
Comparisons of temperature at the geometric center of three layers in wheat flour (water activity 0.45 at 22 °C) during cooling. Temperature data was measured by fiber-optic sensors. Number of replicates (n = 2).

Heating rate	Layer	Temperature (°C)			
		T_{ave} ± SD	T_{max}	T_{min}	ΔT
36.0 °C·min^{-1}	Top	81.6 ± 2.2	85.5	78.4	6.1
	Middle	82.6 ± 1.1	83.9	80.5	
	Bottom	76.5 ± 1.4	78.4	74.1	
11.3 °C·min^{-1}	Top	82.1 ± 0.8	83.1	80.4	4.2
	Middle	82.7 ± 0.8	83.8	80.8	
	Bottom	78.5 ± 1.2	80.1	76.3	
5.5 °C·min^{-1}	Top	78.7 ± 1.0	79.9	76.6	3.4
	Middle	80.2 ± 0.9	81.3	77.9	
	Bottom	76.8 ± 1.4	79.0	74.3	

Table 2
Comparisons of temperature variation (ΔT) and heating uniformity index (UI) of wheat flour (water activity 0.45 at 22 °C) right after RF heating and cooling. Temperature data was measured by thermocouple probes.

Heating rate	Layer	ΔT (°C)	UI after heating	UI after cooling
36.0 °C·min^{-1}	Top	13.5	0.278	0.442
	Middle	9.2	0.238	0.156
	Bottom	8.5	0.203	0.254
11.3 °C·min^{-1}	Top	16.4	0.458	0.399
	Middle	7.8	0.135	0.193
	Bottom	8.2	0.195	0.170
5.5 °C·min^{-1}	Top	15.8	0.465	0.465
	Middle	5.5	0.139	0.143
	Bottom	6.0	0.178	0.120

3.4. Microbial reduction after nature cooling

The population reduction of *E. faecium* increased significantly after the 20 min cooling (Fig. 6). However, the degree of reduction varied among layers and horizontal position. Regardless of the heating rate, the middle layer has the highest microbial reduction, followed by the top and bottom layers. This can be explained by the highest temperature measured in the middle layer. A lower heating rate was helpful to reduce population variance among layers, and this agreed with the results from the heating uniformity study.

At the same heating rate, the microbial reduction varied among different locations in each layer (Fig. 6). For instance, at a heating rate of 36.0 °C·min^{-1}, bacteria at the geometric center (bag No. 1) was inactivated the most for both the top and middle layers, but the least for the bottom layer. A similar inactivation pattern was also observed at a heating rate of 11.3 °C·min^{-1}. However, at a heating rate of 5.5 °C·min^{-1}, bacteria at the right top corner of the container (bag No.5) had the most population reduction for all layers. All bags at the center of the bottom layer (Fig. 6, B1) had the least microbial reduction at all heating rates. The least microbial reduction at the bottom layer might have been the result of the direct contact of the container on the bottom electrode where temperature was at the ambient temperature. The relatively cold electrode caused more rapid temperature reduction of the bottom sample layer, as compared to other parts of the sample, during the natural cooling.

The average log loss of *E. faecium* in each layer is summarized in Fig. 7. The standard division of the average log reduction of *E. faecium* was somewhat high since it was the mean results from five individual packs at the same layer. The edge heating during RF treatment caused the abnormally high-temperature distribution in the corner, in which the No.5 bag was located. From the statistical significance analysis, the log loss of *E. faecium* in the bottom layers after a natural cooling was significantly lower than that from the middle layer regardless of the heating rates. The microbial reduction in the top layer was not significantly different ($P > 0.05$) from that in the bottom layer at a fast heating rate (36 °C·min^{-1}). The log reduction of *E. faecium* in the top layer was significantly lower than that in the middle layer at heating rate 36 °C·min^{-1} and 5.5 °C·min^{-1}.

3.5. Mathematics modeling of survival curves

We used the temperature history obtained from fiber optic sensors to calculate the predicted population reduction of *E. faecium* in wheat flour in different layers. At a different heating rate, the estimated log reduction of *E. faecium* in wheat flour from Bigelow model increased with the extended cooling time (Fig. 8). At the same heating rate, the bottom layers had the constantly lowest microbial reduction of *E. faecium* compared with that from the top and middle layers.

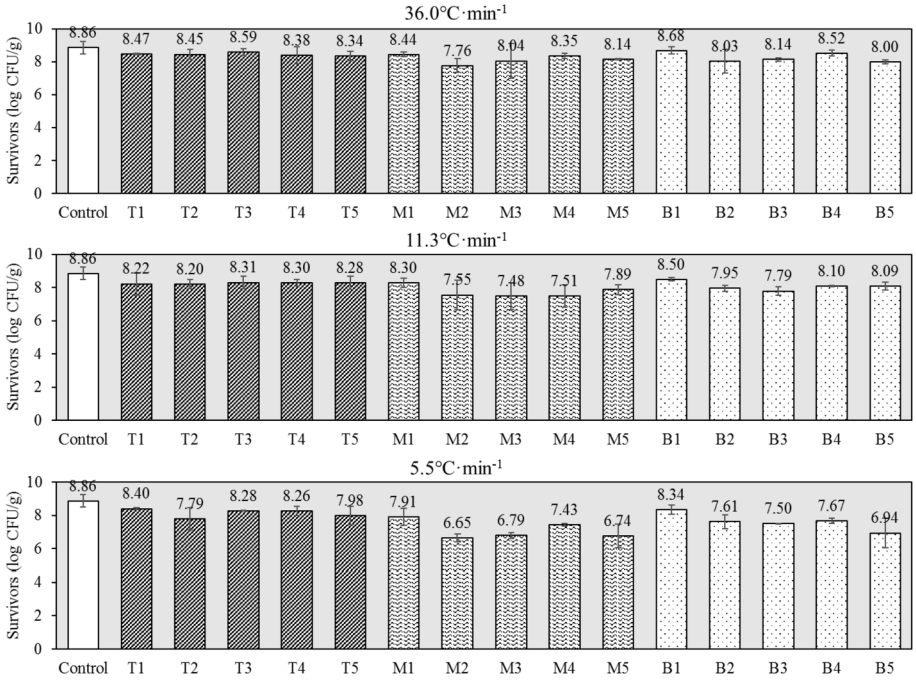

Fig. 5. Survival of *E. faecium* at 15 locations immediately after RF heating at three heating rates (T: top, M: middle, B: bottom layers, number 1–5 indicates the location). Number of replicates (n = 2).

The comparison of microbial reduction from experiment and Bigelow modeled is shown in Table 3. The mean log reductions of *E. faecium* in all cases from the microbiological test were in good agreement (R^2 =0.81) with the predictions from Bigelow model (Fig. 9), assuming *z*-value was 11.7 °C and *D*-value of *E. faecium* was 8.3 min at 80 °C in wheat flour. The reported *D*-value of the same strain at 80 °C in wheat flour (a_w 0.45 at 22 °C) was between 5.56 and 11.80 min (Liu, Ozturk, et al., 2018; Liu, Villas-Rojas et al., 2018) and our fitted *D*-value

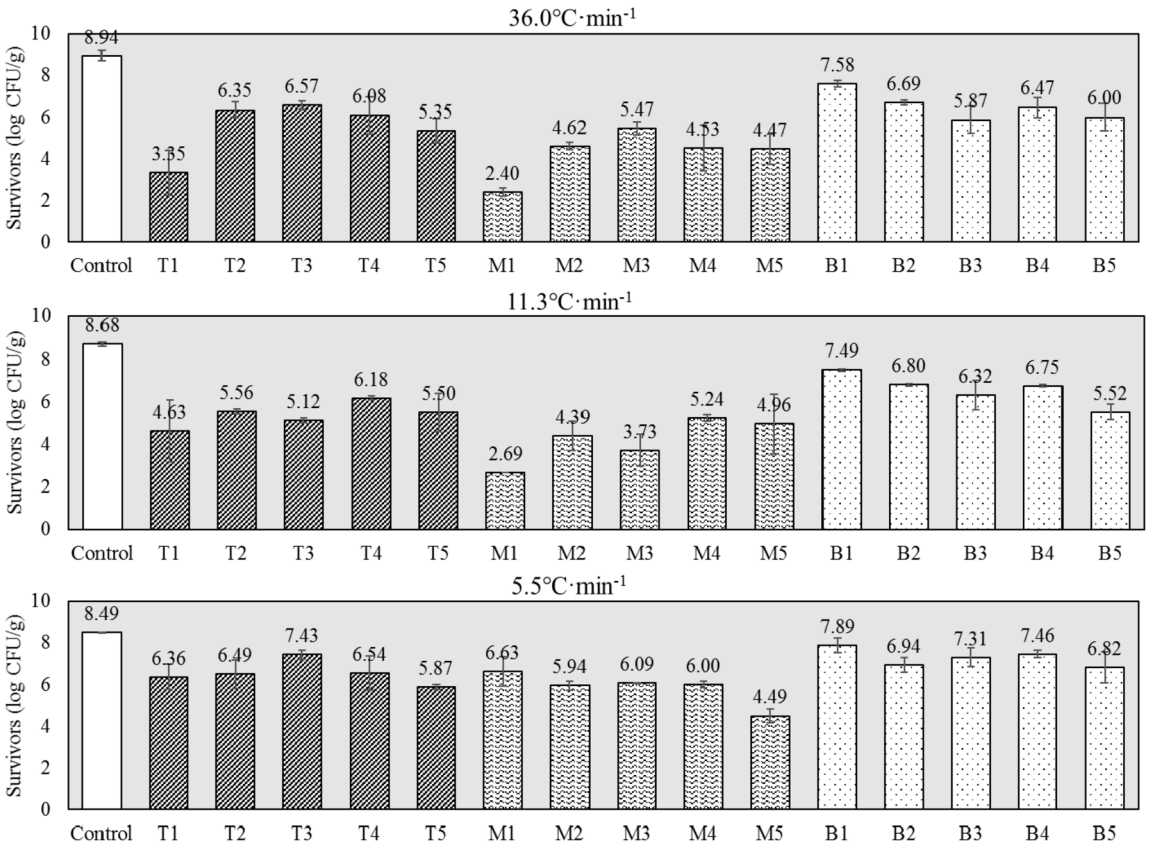

Fig. 6. Survival of *E. faecium* at 15 locations immediately after natural cooling for 20 min under three heating rates (T: top, M: middle, B: bottom layers, number 1–5 indicates the location). Number of replicates (n = 2).

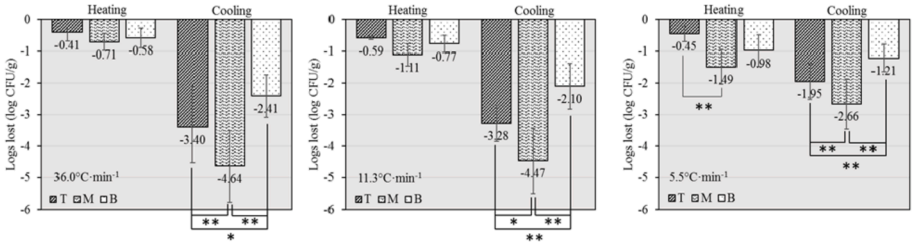

Fig. 7. The average microbial reduction of *E. faecium* at different heating rate during RF process (heating and cooling). (T: top, M: middle, B: bottom layers). Statistical significances of log loss of bacteria in three layers were evaluated respectively. *P > 0.05, **P < 0.05. Number of replicates (n = 2).

fell in that range. In this case, it was fair to claim that the Bigelow model can be used to estimate the real-time microbial reduction of *E. faecium* during RF process by obtaining a temperature history profile at any location of concern.

Since the thermal death of bacteria in wheat flour during RF processing can be predicted by the Bigelow model, it was critical to find the least lethal location after the whole process. Normally, the cold spot of the food matrix in a heating process can be easily identified as the point of least lethality; this method was widely used in the canning industry. The results from this study pointed out that, the slow cooling instead of the short-time heating, was the major contributor to the microbial lethality of RF processed wheat flour or similar products. However, the cold spot may relocate because of heat loss to the environment during the post-RF cooling. In this study, we noticed that the bottom layer always had the lowest temperature compared with the top and middle layer at the end of RF heating (Fig. 4), and this was more obvious at the higher heating rates. During cooling, the heat transfer among layers was not able to relocate the cold spot, which was in the middle of the bottom layer. In another word, the cold spot of this RF process remains to be the spot of least lethality after a 20 min of natural cooling. The temperature variance during cooling was somewhat determined by that during RF heating since the heat conduction among layers during cooling was not obvious based on the temperature profile recorded by the fiber-optic sensors.

During cooling, the heat loss of treated sample had a greater impact on the top and bottom layer compared with that on the middle layer. To maintain a better overall uniformity of thermal treatments, RF heating assisted with a heat convection system (e.g., hot air) is highly recommended. The bottom layer showed the lowest average temperature during RF heating and cooling, and thus, ensuring the container does not have direct contact with the electrode or belt, or warming up the belt before treatment is highly suggested.

4. Conclusion

This study provides a comprehensive approach to validate the application of using Bigelow model to predict the temperature-time dependent microbial reduction of *E. faecium* in RF processes. The results from this study support the application of the Bigelow model for the microbial reduction prediction of RF process on wheat flour at different RF heating rates and different locations of treated samples. The bottom layer, characterized by having the lowest average temperature among three layers, has a significantly low lethality compared with that at the middle layer from both experimental and modeled results. The lowest lethality zone in our experimental setups was located in the center of the bottom layer. This study has provided a strategy to make successful RF processing design for pathogen control in low-moisture foods. A fast-heating rate results in RF non-uniformity in terms of temperature and inactivation. A relatively slow RF heating rate with a hot-air assisted system is helpful to improve the temperature uniformity of RF treatment in order to obtain a uniformed treated sample.

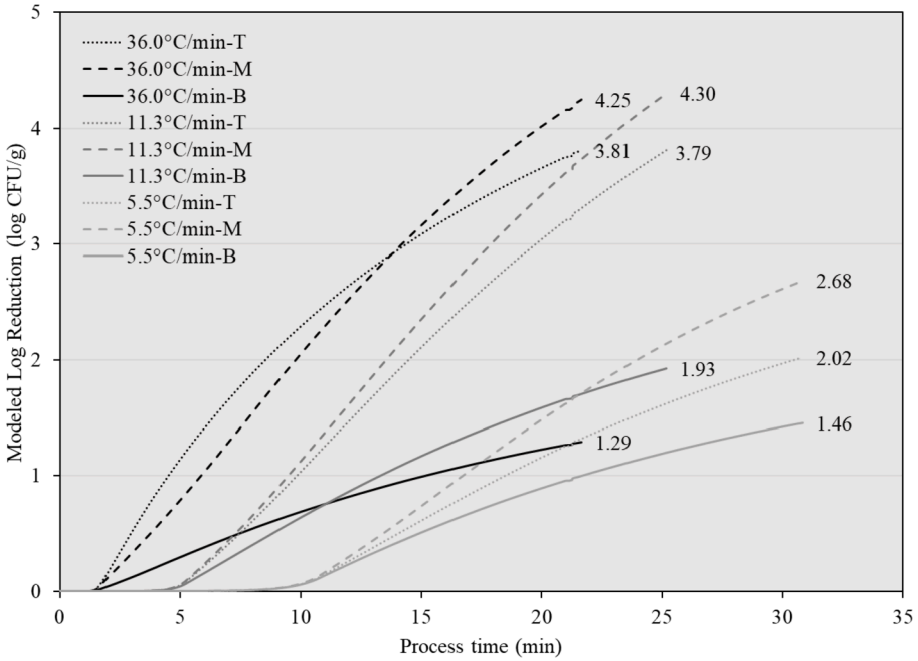

Fig. 8. The real-time microbial reduction of *E. faecium* in wheat flour predicted by Bigelow model when subjected to RF treatment at 80 °C followed by a 20 min natural cooling. (T: top, M: middle, B: bottom layers).

Table 3
Comparison of microbial reduction of *E. faecium* in inoculated-packs from experiment and Bigelow model prediction when subjected to RF heating and a continuous natural cooling at 80 °C for 20 min. Number of replicates (n = 2).

Heating rate	Layer	Microbial reduction from experiment (log CFU/g)	Microbial reduction from Bigelow model (log CFU/g)
36.0 °C·min^{-1}	Top	−3.40 ± 1.31	−3.81
	Middle	−4.64 ± 1.13	−4.25
	Bottom	−2.41 ± 0.68	−1.29
11.3 °C·min^{-1}	Top	−3.28 ± 0.57	−3.81
	Middle	−4.47 ± 1.03	−4.30
	Bottom	−2.10 ± 0.72	−1.93
5.5 °C·min^{-1}	Top	−1.95 ± 0.57	−2.02
	Middle	−2.66 ± 0.80	−2.68
	Bottom	−1.21 ± 0.43	−1.46

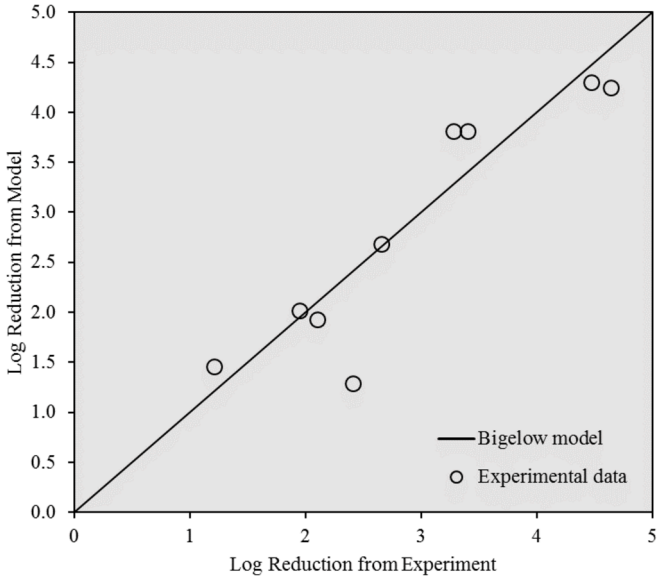

Fig. 9. The fitted line of log reduction of *E. faecium* from Bigelow model and experiment, with R^2 0.81, root mean square 0.5.

Conflicts of interest

The authors declare that they have no conflict of interest.

Acknowledgment

This study was funded by a USDA Agricultural and Food Research Initiative (AFRI)(No. 2015-68003-2341) grant. Authors Jie Xu has received scholarships from the China Scholarship Council. We would like to acknowledge Miles Pepper and Eric Barrow, Voiland College of Engineering and Architecture, Washington State University, for helping us design the temperature measurement system.

References

Alfaifi, B., Tang, J., Rasco, B., Wang, S., & Sablani, S. (2016). Computer simulation analyses to improve radio frequency (RF) heating uniformity in dried fruits for insect control. *Innovative Food Science & Emerging Technologies, 37*(A), 125–137.
Bigelow, W., Bohart, G., Richardson, A., & Ball, C. O. (1920). *Heat penetration in processing canned foods.* Research Laboratory, National Canners Association.
Bigelow, W., & Esty, J. (1920). The thermal death point in relation to time of typical thermophilic organisms. *The Journal of Infectious Diseases,* 602–617.
Birla, S., Wang, S., Tang, J., & Hallman, G. (2004). Improving heating uniformity of fresh fruit in radio frequency treatments for pest control. *Postharvest Biology and Technology, 33*(2), 205–217.
Hildebrandt, I. M., Marks, B. P., Ryser, E. T., Villa-Rojas, R., Tang, J., Garces-Vega, F. J., & Buchholz, S. E. (2016). Effects of inoculation procedures on variability and repeatability of Salmonella thermal resistance in wheat flour. *Journal of Food Protection, 79*(11), 1833–1839.
Hou, L., Kou, X., Li, R., & Wang, S. (2018). Thermal inactivation of fungi in chestnuts by hot air assisted radio frequency treatments. *Food Control, 93*, 297–304.
Huang, Z., Zhu, H., Yan, R., & Wang, S. (2015). Simulation and prediction of radio frequency heating in dry soybeans. *Biosystems Engineering, 129*, 34–47.
Hu, S., Zhao, Y., Hayouka, Z., Wang, D., & Jiao, S. (2018). Inactivation kinetics for *Salmonella* typhimurium in red pepper powders treated by radio frequency heating. *Food Control, 85*, 437–442.
Jiao, S., Johnson, J., Tang, J., & Wang, S. (2012). Industrial-scale radio frequency treatments for insect control in lentils. *Journal of Stored Products Research, 48*, 143–148.
Jiao, Y., Shi, H., Tang, J., Li, F., & Wang, S. (2015). Improvement of radio frequency (RF) heating uniformity on low moisture foods with Polyetherimide (PEI) blocks. *Food Research International, 74*, 106–114.
Jiao, Y., Tang, J., & Wang, S. (2014). A new strategy to improve heating uniformity of low moisture foods in radio frequency treatment for pathogen control. *Journal of Food Engineering, 141*, 128–138.
Kim, S.-Y., Sagong, H.-G., Choi, S. H., Ryu, S., & Kang, D.-H. (2012). Radio-frequency heating to inactivate *Salmonella* typhimurium and *Escherichia coli* O157: H7 on black and red pepper spice. *International Journal of Food Microbiology, 153*(1), 171–175.
Li, R., Kou, X., Cheng, T., Zheng, A., & Wang, S. (2017). Verification of radio frequency pasteurization process for in-shell almonds. *Journal of Food Engineering, 192*, 103–110.
Liu, S., Ozturk, S., Xu, J., Kong, F., Gray, P., Zhu, M.-j., et al. (2018a). Microbial validation of radio frequency pasteurization of wheat flour by inoculated pack studies. *Journal of Food Engineering, 217*, 68–74.
Liu, S., Rojas, R. V., Gray, P., Zhu, M.-J., & Tang, J. (2018b). *Enterococcus faecium* as a *Salmonella* surrogate in the thermal processing of wheat flour: Influence of water activity at high temperatures. *Food Microbiology, 74*, 92–99.
Liu, S., Tang, J., Tadapaneni, R. K., Yang, R., & Zhu, M.-J. (2018c). Exponentially increased thermal resistance of *Salmonella* spp. and *Enterococcus faecium* at reduced water activity. *Applied and Environmental Microbiology, 84*(8) e02742-02717.
Mermelstein, N. H. (1998). Microwave and radiofrequency drying. *Food Technology, 52*(11), 84–86.
Niebuhr, S., Laury, A., Acuff, G., & Dickson, J. (2008). Evaluation of nonpathogenic surrogate bacteria as process validation indicators for *Salmonella* enterica for selected antimicrobial treatments, cold storage, and fermentation in meat. *Journal of Food Protection, 71*(4), 714–718.
Ozturk, S., Kong, F., Singh, R. K., Kuzy, J. D., & Li, C. (2017). Radio frequency heating of corn flour: Heating rate and uniformity. *Innovative Food Science & Emerging Technologies, 44*, 191–201.
Ozturk, S., Kong, F., Trabelsi, S., & Singh, R. K. (2016). Dielectric properties of dried vegetable powders and their temperature profile during radio frequency heating. *Journal of Food Engineering, 169*, 91–100.
Piyasena, P., Dussault, C., Koutchma, T., Ramaswamy, H., & Awuah, G. (2003). Radio frequency heating of foods: Principles, applications and related properties—a review. *Critical Reviews in Food Science and Nutrition, 43*(6), 587–606.
Podolak, R., & Black, D. G. (2017). *Control of Salmonella and other bacterial pathogens in low-moisture foods.* John Wiley & Sons.
Syamaladevi, R. M., Tang, J., Villa-Rojas, R., Sablani, S., Carter, B., & Campbell, G. (2016). Influence of water activity on thermal resistance of microorganisms in low-moisture foods: A review. *Comprehensive Reviews in Food Science and Food Safety, 15*(2), 353–370.
Tiwari, G., Wang, S., Tang, J., & Birla, S. (2011). Computer simulation model development and validation for radio frequency (RF) heating of dry food materials. *Journal of Food Engineering, 105*(1), 48–55.
Villa-Rojas, R. (2015). *Influence of different factors on desiccation survival and thermal resistance of Salmonella and radiofrequency pasteurization of low-moisture foods*Dissertation. Washington State University.
Villa-Rojas, R., Tang, J., Wang, S., Gao, M., Kang, D. H., Mah, J. H., et al. (2013). Thermal inactivation of *Salmonella* enteritidis PT 30 in almond kernels as influenced by water activity. *Journal of Food Protection, 76*(1), 26–32.
Villa-Rojas, R., Zhu, M.-J., Marks, B. P., & Tang, J. (2017). Radiofrequency inactivation of *Salmonella* Enteritidis PT 30 and *Enterococcus faecium* in wheat flour at different water activities. *Biosystems Engineering, 156*, 7–16.
Wang, S., Monzon, M., Johnson, J., Mitcham, E., & Tang, J. (2007a). Industrial-scale radio frequency treatments for insect control in walnuts: I: Heating uniformity and energy efficiency. *Postharvest Biology and Technology, 45*(2), 240–246.
Wang, S., Monzon, M., Johnson, J., Mitcham, E., & Tang, J. (2007b). Industrial-scale radio frequency treatments for insect control in walnuts: II: Insect mortality and product quality. *Postharvest Biology and Technology, 45*(2), 247–253.
Wang, S., Tiwari, G., Jiao, S., Johnson, J., & Tang, J. (2010). Developing postharvest disinfestation treatments for legumes using radio frequency energy. *Biosystems Engineering, 105*(3), 341–349.
Wei, X. (2017). *Radiofrequency processing for inactivation of Salmonella spp. and Enterococcus faecium NRRL B-2354 in whole black peppercorn and ground black pepper*Dissertation. University of Nebraska-Lincoln.
Xu, J., Liu, S., Tang, J., Ozturk, S., Kong, F., & Shah, D. H. (2018). Application of freeze-dried *Enterococcus* faecium NRRL B-2354 in radio-frequency pasteurization of wheat flour. *LWT-Food Science and Technology, 90*, 124–131.
Xu, J., Tang, J., Jin, Y., Song, J., Yang, R., Sablani, S. S., et al. (2018). High temperature water activity as a key factor influencing survival of *Salmonella* Enteritidis PT30 in thermal processing. *Food Control, 98*, 520–528.
Zhang, P., Zhu, H., & Wang, S. (2015). Experimental evaluations of radio frequency heating in low-moisture agricultural products. *Emirates Journal of Food and Agriculture,* 662–668.
Zheng, A., Zhang, L., & Wang, S. (2017). Verification of radio frequency pasteurization treatment for controlling *Aspergillus* parasiticus on corn grains. *International Journal of Food Microbiology, 249*, 27–34.